

Sterile Neutrino Decays and Constraints on the Flux of $\bar{\nu}_e$ from the Sun

Matheus Hostert^{1,2,3,*} and Maxim Pospelov^{1,2,3,†}

¹*School of Physics and Astronomy, University of Minnesota, Minneapolis, MN 55455, USA*

²*William I. Fine Theoretical Physics Institute, School of Physics and Astronomy,
University of Minnesota, Minneapolis, MN 55455, USA*

³*Perimeter Institute for Theoretical Physics, Waterloo, ON N2J 2W9, Canada*

(Dated: December 11, 2019)



Searches for solar antineutrinos from $\nu \rightarrow \bar{\nu}$ conversions of B^8 neutrinos are highly sensitive to any source of MeV antineutrinos from the Sun. In this work we adapt these searches to non-minimal sterile neutrino models recently proposed to explain the LSND, MiniBooNE, and reactor anomalies. The production of such sterile neutrinos in the Sun, followed their cascade-like decays $\nu_4 \rightarrow \nu\varphi \rightarrow \nu\nu\bar{\nu}$ via a new scalar φ results in sub-per-mille upper limits for the neutrino mixing $|U_{e4}|^2$. We conclude that a simultaneous explanations of all anomalies is in tension with KamLAND, Super-Kamiokande, and Borexino data. Future searches with a Gadolinium-doped Super-Kamiokande tank is expected to improve on our results. Finally, we comment on a novel possibility to constrain sterile neutrino secret interactions by considering the impact of number-changing processes of the type and $\nu\nu \rightarrow \nu\nu\varphi$ on the detection of supernova neutrinos from SN1987A.

I. INTRODUCTION

The Mikheyev-Smirnov-Wolfenstein (MSW) [1, 2] solution to the solar neutrino problem played a pivotal role in the discovery that neutrinos have masses and mix [3, 4]. Beyond neutrino mixing, the study of solar neutrinos provides important inputs to the Standard Solar Model (SSM) [5] and may be used to search for physics beyond the Standard Model (SM) of particle physics [6]. Indeed, after precision measurements of the solar neutrino oscillation parameters by KamLAND [7], one can derive strong constraints on a variety of new physics scenarios, such as models with enhanced decays of ν_2 and ν_3 [8, 9], originally proposed as an alternative solution to the solar neutrino problem [10, 11]. Although such scenarios are constrained very effectively due to the astronomical distances travelled by solar neutrinos and our precise knowledge of the Sun's interior from helioseismic probes, yet another feature explored in the literature is important for new physics searches. The flux of antineutrinos from the Sun at the MeV energies is negligible [12], which remains an excellent approximation down to tens of keV in energy [13]. Combined with the larger detection cross section for $\bar{\nu}_e$ compared to that of ν_e , this makes solar neutrino experiments sensitive to very small fluxes of antineutrinos [14, 15]. Quantitatively, the current sensitivity reaches fluxes as small as a few *hundred-thousandths* of the 8B neutrino flux [16–19].

A simple scenario for a new physics source of solar antineutrinos is given by $\nu \rightarrow \bar{\nu}$ oscillations. As it turns out, this Lepton number (LN) violating process is rather small as it is suppressed by $(m_\nu/E)^2$. However, such LN violating signature can also be realised through neutrino

decay. For instance, neutrino mass models where LN is a spontaneously broken global symmetry predict the existence of a pseudo-goldstone boson J , the majoron [20, 21]. In these models, solar (and supernova) antineutrinos may be produced from the decay $\nu_2 \rightarrow \bar{\nu}_1 J$, which is enhanced in matter [22]. This possibility of production from neutrino decay is, in fact, quite general and can be realised in any LN violating model with neutrinos that decay sufficiently fast, be they ν_2 , ν_3 , or a new mostly-sterile state ν_4 (see Ref. [23] for an early discussion in the context of a 17 keV sterile neutrino). Another source of $\nu \rightarrow \bar{\nu}$ conversion is spin-flavour precession [24, 25], where the coupling of a large neutrino magnetic moment to the solar magnetic field induces $\nu_e \rightarrow \bar{\nu}_\mu$ conversions, which subsequently converts to $\bar{\nu}_e$ due to matter effects.

Here we focus on a different possibility. Our work is motivated by a variety of proposals to explain the anomalous $\nu_\mu \rightarrow \nu_e$ appearance results at short-baseline neutrino experiments with so-called visible sterile neutrino decays [26–30]. These models introduce a sterile neutrino field to the SM, ν_s , which has large couplings to active neutrinos via a new scalar particle φ ¹. This can be done in a gauge invariant way by coupling the new mediator purely to ν_s and admitting large mixing between the heaviest neutrino state, ν_4 , and the active flavours. Independently of the underlying model, the explanation of anomalous $\nu_\mu \rightarrow \nu_e$ appearance at short-baselines relies on the sequence of decays $\nu_4 \rightarrow \nu_e\varphi \rightarrow \nu_e\nu_e\bar{\nu}_e$. In the Sun, such eV-keV sterile neutrinos lead to large numbers of antineutrinos, in contradiction with null results for solar antineutrino searches. Given that, we derive limits on the electron and muon flavour mixing with ν_4 , working only with the gauge-invariant and parity-conserving model of Ref. [29]. We focus solely on Dirac neutrinos, as

* mhostert@umn.edu

†

¹ In Appendix A we show that our conclusions hold also for models where a vector particle is introduced instead.

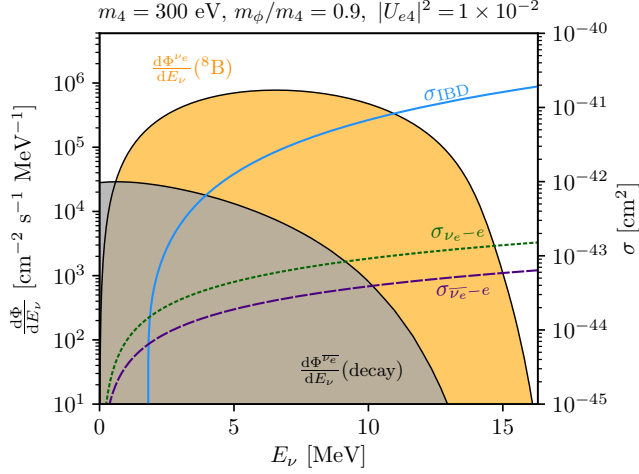


FIG. 1. The solar neutrino energy spectrum from 8B (shaded orange) and from the decays of ν_4 (shaded grey). We also show the inverse beta decay (IBD) and neutrino-electron scattering cross sections on an overlaid axis.

our bounds are very strong in that limit, excluding most of the parameter space preferred by the short-baseline anomalies in this case. For models with Majorana neutrinos, they become even stronger due to $\nu_4 \rightarrow \bar{\nu}\varphi \rightarrow \nu\bar{\nu}$ decays. The only relevant possibility not covered by our bounds is that of Dirac neutrinos interacting with a massless boson. Nevertheless, we point out that any model with large neutrino self-interactions via new light mediators faces a challenge to explain the observed neutrino events from SN1987A [31, 32]. Differently from usual arguments of energy-loss via the emission of invisible particles, we argue that a large rate of number-changing processes would efficiently cool the supernova neutrino gas.

The paper is organized as follows...

II. FAST STERILE NEUTRINO DECAYS

A. Short-Baseline Anomalies

B. The Model

The SM is extended by the following Lagrangian

$$-\mathcal{L} = g_\varphi \bar{\nu}_s \nu_s \varphi + \sum_{\alpha, \beta} m_{\alpha\beta} \bar{\nu}_\alpha \nu_\beta, \quad (1)$$

where the neutrino mass mechanism is left unspecified and assumed to not play a role in our discussion. In the mass basis, the neutrino mass eigenstates are given by $\nu_i = \sum_\alpha U_{\alpha i} \nu_\alpha$, with U the unitary mixing matrix. In the decays of ν_4 , only the three lightest mass states are produced, and so it is useful to define $\nu_F = \sum_i U_{si} \nu_i$.

Due to mixing, sterile neutrinos with masses below the MeV would be produced in the Sun via the same

processes responsible for ν_e production at a rate $|U_{e4}|^2$ times smaller. Once produced, the ν_4 mass eigenstates immediately decay to a massless neutrino and a boson, which may be a scalar or a vector boson. The boson then promptly decays to a neutrino-antineutrino pair, giving rise to our signal. Overall, the process of interest is

$$\begin{aligned} \nu_4(E_\nu) &\rightarrow \nu_e(E_1) + \varphi(E_\varphi) \\ &\searrow \nu_e(E_2) + \bar{\nu}_e(E_3). \end{aligned} \quad (2)$$

We now summarise the decay rates for a heavy Dirac neutrino decaying to an active neutrino flavour, and a scalar φ . The heavy neutrino is assumed to be polarised with a definite helicity h . For most cases of interest, $E_\nu \gg m_4$, so if ν_4 is produced in Weak interactions, the right-handed ν_4 population is negligible. Nevertheless, due to the assumption of parity conservation for the φ interactions with neutrinos, one can compute the helicity flipping (HF) and helicity conserving (HC) decay channels by noting that

$$\begin{aligned} d\Gamma(\nu_4^{h=-1} \rightarrow \nu_L \varphi) &= d\Gamma(\nu_4^{h=1} \rightarrow \nu_R \varphi), \\ d\Gamma(\nu_4^{h=1} \rightarrow \nu_L \varphi) &= d\Gamma(\nu_4^{h=-1} \rightarrow \nu_R \varphi). \end{aligned} \quad (3)$$

In this way, all HF decay rates are given by $d\Gamma(\nu_4^{h=1} \rightarrow \nu_L \varphi)$ and all HC channels by $d\Gamma(\nu_4^{h=-1} \rightarrow \nu_L \varphi)$. Assuming all neutrinos to be ultra-relativistic, we find the squared-amplitudes for $\nu_4^h \rightarrow \nu_L^h \varphi$ to leading order in the small mixing elements as shown below,

$$|\mathcal{M}_h|^2 = g_\varphi^2 |U_{\alpha 4}|^2 \frac{m_4^2}{2} \left[(1+h)(1-r^2) - 2h \frac{E_1}{E_\nu} \right], \quad (4)$$

where $r = m_\varphi/m_4$. Integrated over phase space, both channels contribute identically to a total decay rate of

$$\Gamma^{\text{LAB}}(\nu_4 \rightarrow \nu_\alpha \varphi) = \frac{g_\varphi^2}{16\pi} \frac{m_4^2}{E_\nu} |U_{\alpha 4}|^2 (1-r^2)^2, \quad (5)$$

Our decay rate is in agreement with Refs [29, 33]. Note that helicity conserving decays prefer larger E_1 values, while helicity flipping decays prefer smaller values of E_1 . Therefore, for our present application, helicity-flipping decays are important since the antineutrinos from the subsequent scalar decay tend to be more energetic. In the limit $r \rightarrow 1$, the scalar field has virtually all of the ν_4 energy regardless of the helicity structure of the decay, and so it is the scenario most easily constrained by our analysis.

For completeness, we also show the scalar decay length in the lab frame to leading order in the small mixing elements

$$\Gamma^{\text{LAB}}(\varphi \rightarrow \nu_\alpha \nu_\beta) = \frac{g_\varphi^2}{8\pi} \frac{m_\varphi^2}{E_\varphi} |U_{\alpha 4}|^2 |U_{\beta 4}|^2. \quad (6)$$

Note that the scalar decays are doubly suppressed by small mixing elements, and so it tends to decay more slowly than the heavy neutrinos. Nevertheless, the decay of both particles can be considered prompt for all parameters of interest.

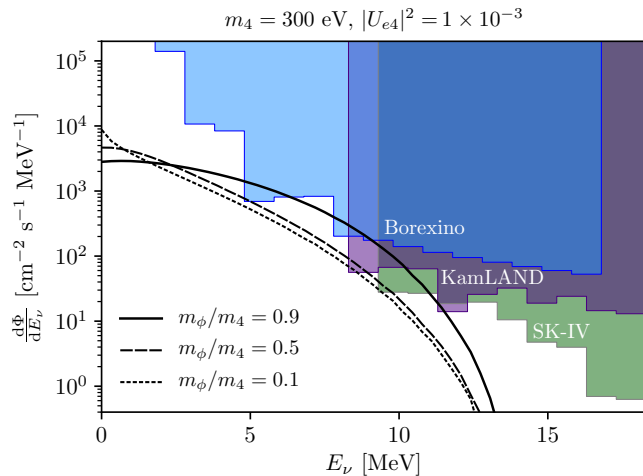


FIG. 2. The experimental limits on solar $\bar{\nu}_e$ at 90% C.L. as a function of the neutrino energy. The shaded regions are excluded by Borexino (blue), KamLAND (purple) and SuperK-IV (grey). Three different new physics predictions are also shown as solid curves assuming $|U_{\mu 4}| = |U_{\tau 4}| = 0$.

III. SOLAR ANTINEUTRINOS

The flux of MeV antineutrinos from the Sun in the SSM is negligibly small. The largest antineutrino flux at MeV energies comes from small fractions of long-lived radioactive isotopes in the Sun, namely ^{232}Th , ^{238}U , and mainly ^{40}K . Ignoring flavour effects, this give rise to a $\bar{\nu}_e$ flux on Earth of about $200 \text{ cm}^{-2} \text{ s}^{-1}$ with $E_\nu \lesssim 3 \text{ MeV}$ [12]. This component, however, is still 6 orders of magnitude smaller than the geoneutrino flux at the surface of the Earth at these energies, and can be safely neglected. At larger energies, photo-fission reactions produce an even smaller flux of $\bar{\nu}_e$ of about $10^{-3} \text{ cm}^{-2} \text{ s}^{-1}$ [12]. It is only down at the much lower energies of tens of keV that antineutrinos start being produced in thermal reactions at a similar rate to neutrinos with fluxes as large as $10^9 \text{ cm}^{-2} \text{ s}^{-1}$ [13].

Solar antineutrinos have been searched for at various solar neutrino experiments. The most stringent upper limits on an undistorted flux of solar $\bar{\nu}_e$ from ^8B are given by KamLAND [17]

$$P_{\nu_e \rightarrow \bar{\nu}_e}^{\text{KamLAND}}(E_\nu \geq 8.3 \text{ MeV}) < 5.3 \times 10^{-5}, \quad (7)$$

and Borexino [18]

$$P_{\nu_e \rightarrow \bar{\nu}_e}^{\text{Borexino}}(E_\nu \geq 1.8 \text{ MeV}) < 7.2 \times 10^{-5}, \quad (8)$$

both at 90% C.L. SuperKamiokande (SK) has derived limits on extraterrestrial $\bar{\nu}_e$ sources during phases I, II and III [34], but the high energies of $E_\nu > 17.3 \text{ MeV}$ are irrelevant for the study of B^8 neutrinos. For SK phase IV, improvements to the trigger system were implemented and neutron tagging was then possible, lowering thresholds to 13.3 MeV [35]. Recently, further improvements

to the neutron tagging algorithm lowered this value to $E_\nu > 9.3 \text{ MeV}$, which was then used to analyse all SK phase IV (SK-IV) data in a preliminary study [19]. Interpreting the results of the latter study as 90% C.L. upper limits on $P_{\nu_e \rightarrow \bar{\nu}_e}$, we find

$$P_{\nu_e \rightarrow \bar{\nu}_e}^{\text{SK-IV}}(E_\nu \geq 9.3 \text{ MeV}) \lesssim 1.0 \times 10^{-4}. \quad (9)$$

In addition to these, SNO has also set limits at the level of $P_{\nu_e \rightarrow \bar{\nu}_e}^{\text{SNO}}(E_\nu \in [4, 14.8] \text{ MeV}) < 8.3 \times 10^{-3}$ [16] at 90% C.L. All limits quoted here assume a total ^8B flux of $5.94 \times 10^6 \text{ cm}^{-2} \text{ s}^{-1}$. At the lowest energies, a bound can also be obtained by noting that the number of elastic $\nu - e$ scattering events in solar neutrino experiments decreases if too many ν_4 states are produced, both due to lower $\bar{\nu}_e - e$ cross sections and suppressed ν_e flux. These effects, however, are insensitive to variations of the total ν_e flux below the few percent level. The model independent bounds quoted by KamLAND, Borexino and SK-IV are shown in Fig. 2.

The strength of the above limits is due to the large cross section for Inverse beta decay (IBD) of free protons at MeV electron-antineutrinos energies. Beyond dominating over the neutrino-electron elastic scattering cross section by about two orders of magnitude (see Fig. 1), this channel has a distinct signature that drastically reduces backgrounds. After produced, the positron annihilates and the final state neutron is quickly captured by the free protons. This results in a double-bang signal with a positron kinetic energy $T_e = E_\nu - 1.8 \text{ MeV}$, and a delayed emission of a $\approx 2.2 \text{ MeV}$ gamma. The cross section for this process is well understood at high [36] and low [37] energies, and relatively simple formulae that are valid for all energy regimes have been derived by Ref. [38]. In this work we implement the latter calculation, which is provided as machine-friendly data files by Ref. [39].

A. Backgrounds

For Borexino, reactor neutrino represent the largest source of backgrounds, but are effectively constrained by DayaBay measurements. Atmospheric neutrino events with genuine IBD scattering or otherwise inherit large uncertainties from the atmospheric neutrino flux and cross sections, but represent only a small contribution (6.5 ± 3.2 events). Finally, the U^{238} and Th^{232} geoneutrino fluxes are energetic enough to contribute to the IBD sample, but are only significant up to 3.2 MeV. Borexino omits the contribution of geoneutrinos from the Earth's mantle in their estimation, which is conservative. This component is the most likely explanation for the $\approx 2\sigma$ excess seen in the lowest energy bin [18].

The reactor neutrino flux at KamLAND is dominant below 8.3 MeV, but contributes only about 2.2 events above that value. Due to the smaller meter water equivalent overburden at KamLAND and SK, they suffer from larger spallation backgrounds, coming mainly from radioactive decays of Li^9 . After muon tagging and fiducial

volume cuts, these are reduced to less than 5 events at both locations.

The large number of neutrino-electron scattering events presents a background to SK. For this reason, a cut is applied requiring $\cos \theta. < 0.9$. This does not impact IBD events as the positron angle with respect to the incoming neutrino is significantly larger ($\langle \cos \theta \rangle \approx -0.01$) than in the predominantly forward process of elastic scattering.

B. Decaying-Sterile Signal

To leading order in the small mixing angles, the number of IBD events in a given experiment can be computed as

$$\frac{dN_{\text{events}}}{dE_\nu dE_1 dE_3} = \mathcal{N} \frac{d\Phi^{\nu_4}}{dE_\nu} \frac{dP^{\text{dec}}}{dE_1 dE_3} \sigma^{\text{IBD}}(E_3) \overline{P_{ee}}(E_3), \quad (10)$$

where \mathcal{N} stands for total exposure of the experiment and

$$\begin{aligned} \frac{d\Phi^{\nu_4}}{dE_\nu} &= |U_{e4}|^2 \frac{d\Phi^{\nu_e}}{dE_\nu}, \\ \frac{dP^{\text{dec}}}{dE_1 dE_3} &= \frac{1}{\Gamma_{\nu_h} \Gamma_{Z'}} \frac{d\Gamma_{\nu_h \rightarrow \nu_e Z'}}{dE_1} \frac{d\Gamma_{Z' \rightarrow \nu_e \bar{\nu}_e}}{dE_2}. \end{aligned} \quad (11)$$

Note that Eq. (10) is the analogue of Eq. (18) from Ref. [29], and is simpler since we work with very long baselines and under the assumption that the number of initial ν_μ states is negligible.

IV. RESULTS AND FUTURE PROSPECTS

Solar antineutrino searches are likely to become even more stringent with upcoming efforts to detect antineutrinos from the diffuse supernova neutrino background (DSNB) [40, 41]. For instance, the SK detector is expected to detect this neutrino flux when Gadolinium is added to its active volume [42]. The large neutron capture cross sections by Gd and the emission of 8 MeV gammas will help reduce backgrounds and lower the $\bar{\nu}_e$ detection threshold to neutrino energies as low as the IBD threshold, provided $E_e > 0.8$ MeV [43]. The increased detection efficiencies at lower energies and reduced accidental and mis-reconstructed backgrounds are bound to improve on the limits we set on heavy neutrino decays. In addition, with the detection of the DSNB, one may also constrain the models considered here by looking for dips in the DSNB spectrum due to interactions the relic neutrinos [44].

As pointed out by Li *et al* [45], future large liquid scintillator detectors, such as the Jiangmen Underground Neutrino Observatory (JUNO) [46] and the Jinping neutrino experiment [47], will likely also be able to improve on current bounds of solar antineutrinos with $E_\nu \gtrsim 8.5$ MeV, and offer yet another opportunity to improve upon our limits.

V. SUPERNOVA NEUTRINOS

The detection of neutrinos from SN1987A by the Kamiokande-II [32] and IMB [31] experiments provide insights to the interior of core-collapse supernovae. These water-cherenkov experiments observed a total of 19 supernova neutrino events in a time period of 13 s. This has been explored in the literature to constrain new physics in the neutrino sector, mainly in the context of majoron models. Constraints on the majoron coupling to light neutrinos have been derived from arguments about energy loss and time duration of the supernova neutrino signal [], although such constraints suffer from uncertainties in the modelling of the supernova core and the explosion mechanism. In the decaying-sterile model of Ref. [29], both the heavy neutrino and its accompanying scalar have relatively large couplings to neutrinos and remain trapped inside the core. Although this precludes constraints from energy loss arguments, it introduces other problems. The large couplings keep neutrinos (light and heavy), as well as φ , in thermal equilibrium for much larger radii, much beyond the radius where neutrinos decouple from the ordinary supernova matter. Of particular significance are the number-changing processes of the type

$$\nu\nu \rightarrow \nu\nu\varphi, \varphi\varphi\varphi \quad (12)$$

$$\nu\varphi \rightarrow \nu\nu\nu, \nu\varphi\varphi, \quad (13)$$

$$\varphi\varphi \rightarrow \varphi\nu\nu, \quad (14)$$

which efficiently cool the neutrino gas as it propagates outwards.

In the ultra-relativistic limit, one can find an order of magnitude estimate for the cross section of process the bremsstrahlung process $\nu\nu \rightarrow \nu\nu\varphi$ using [48]

$$\frac{d\sigma_{\nu\nu \rightarrow \nu\nu\varphi}}{dx_\varphi} \approx |U|^{2n} \sigma_{\nu\nu \rightarrow \nu\nu} \frac{\alpha_\varphi}{\pi} \frac{1}{x_\varphi} \left[\ln \frac{s(1-x_\varphi)}{m^2} - 1 \right], \quad (15)$$

where $\alpha_\varphi = g_\varphi^2/4\pi$, $s = (p_1 + p_2)^2$, $x_\varphi = 1 - (k_1 + k_2)^2/s$, and m is the mass of the outgoing neutrinos. We factor the small active-heavy mixing element $|U|$ out of the scattering cross section $\sigma_{\nu\nu \rightarrow \nu\nu}$, where n counts the number of light neutrinos (ν_i , $i = 1, 2$ and 3) in the external legs. The same power counting of $|U|$ arises in the processes (12) and (13). One can easily see that with large couplings g and mixings of the order of $|U|^2 \sim 10^{-3}$, as required by the short-baseline anomalies, the total cross section for the bremsstrahlung of φ in $\nu_\alpha \nu_\beta \rightarrow \nu_\alpha \nu_\beta \varphi$, for instance, can be as large as 10^{-27} cm^2 . Although a dedicated analysis is in order, one can already deduce that such efficient processes will cool the neutrino-scalar gas to much lower temperatures ($T < ? \text{ MeV}$), also delaying the neutrino emission. This would be in stark contradiction with the detection of SN1987A neutrinos. We emphasise that a dedicated analysis is needed before any

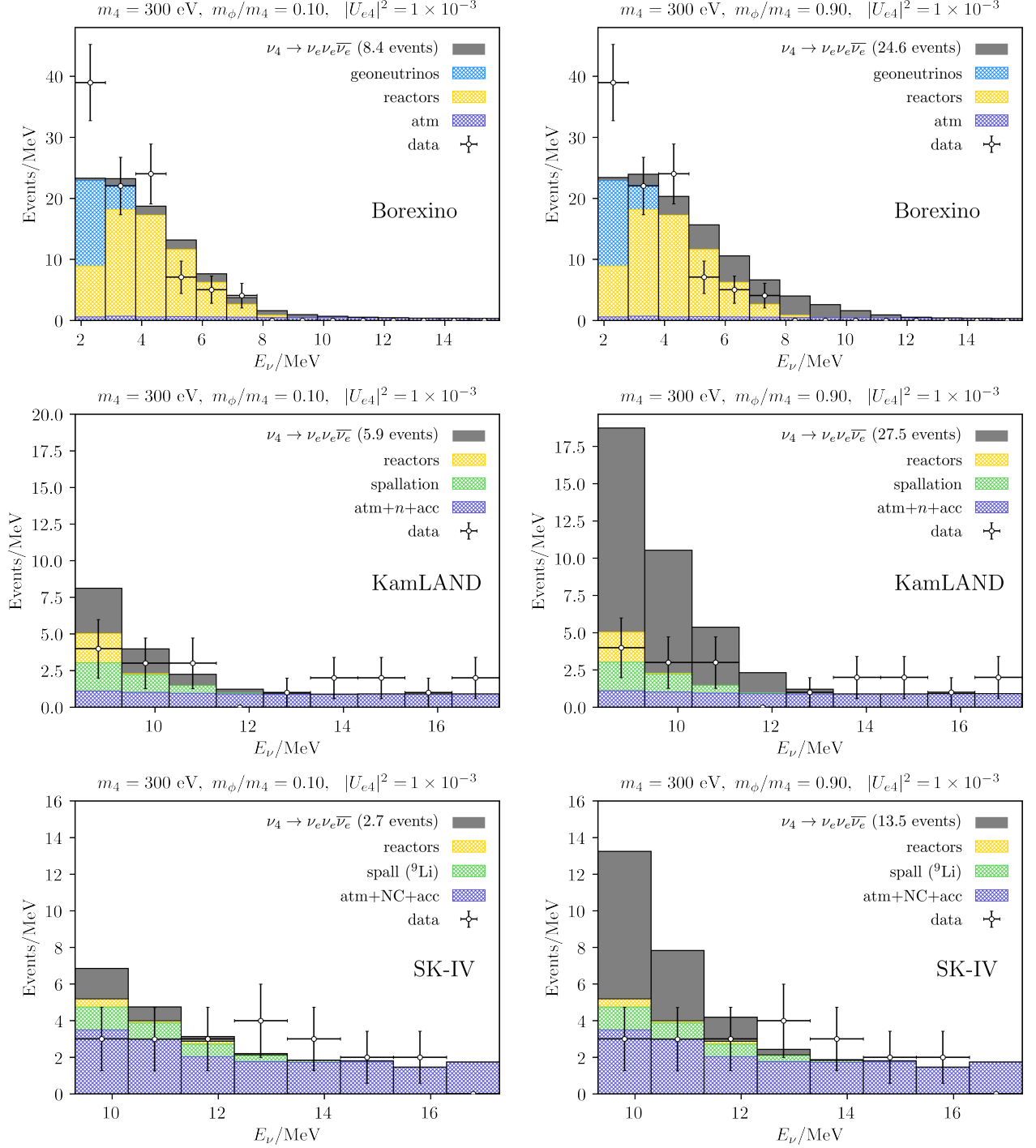


FIG. 3. The inverse beta decay spectrum at KamLAND (top row) and Borexino (bottom row) as stacked histograms. The filled histograms show the background estimations by the collaboration, and the hashed histogram the prediction of visible neutrino decays. For KamLAND, we also show the 90% C.L. upper limit on the event spectra provided by the collaboration. All plots assume $|U_{\mu 4}| = |U_{\tau 4}| = 0$.

constraints can be set ², but that our arguments apply

² Such effects would also be present in the inner layers of the core,

but a conservative statement can be made about the neutrino-scalar gas expansion beyond the neutrinosphere.

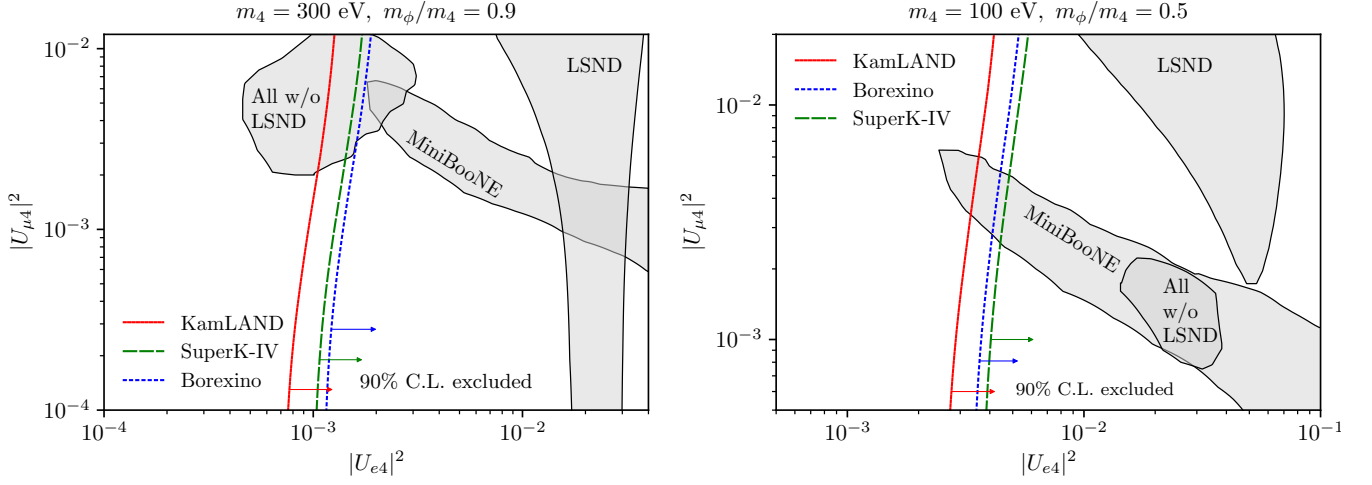


FIG. 4. Solar neutrino experiment limits on the mixing angles required to explain the short-baseline anomalies. The shape of the curve is explained by the BR of φ into final state neutrinos.

for a large class of neutrino self-interactions through light bosons, including the so-called invisible sterile neutrino decays, also proposed as an alternative solution to the short-baseline anomalies [28, 49, 50].

VI. CONCLUSIONS

ACKNOWLEDGMENTS

The authors would like to thank Linyan Wan for useful comments on the SuperKamiokande-IV searches and Carlos Argüelles for discussions on the nusQUIDS code. This research was supported in part by Perimeter Institute for Theoretical Physics. Research at Perimeter Institute is supported by the Government of Canada through the Department of Innovation, Science and Economic Development and by the Province of Ontario through the Ministry of Research, Innovation and Science.

Appendix A: Vector case

Our bounds also apply to the case where sterile neutrinos decay to vector particles. A model for such scenarios can be built in a very similar way to the scalar case, although cosmological constraints on such vector states are in general harder to avoid [51]. Nevertheless, take a simplified model with new interactions due to a new vector boson X^μ as follows

$$\mathcal{L} = m_X X_\mu X^\mu - g_X X_\mu \bar{\nu}_s \gamma^\mu \nu_s - \sum_{\alpha, \beta} m_{\alpha\beta} \bar{\nu}_\alpha \nu_\beta. \quad (\text{A1})$$

Then, the amplitude for the decay $\nu_4^h \rightarrow \nu_L^\alpha X$ is given by

$$|\mathcal{M}_h|^2 = g_X^2 |U_{\alpha 4}|^2 \frac{m_4^2 (1 - r^2)}{2r^2} \left[(1 - h) 2r^2 + (1 + h) - 2h \frac{E_1}{E_\nu} \frac{1 - 2r^2}{1 - r^2} \right], \quad (\text{A2})$$

where $r = m_X/m_4$. From this, one finds a spectrum of final state particles which is very similar to the scalar case. Such secret interactions can be accommodated by lowering the new scales in the models proposed by Refs. [51, 52]).

Appendix B: Solar Flavour Transitions

Once produced from the ν_4 decay, the active neutrinos propagate from the Sun's core to the Earth, subject to matter effects. The flavour evolution of these neutrinos is given by the well-known LMA-MSW solution. Here, we are primarily interested in the total $\bar{\nu}_e$ flux that exits the Sun, so all antineutrinos produced in the decay of the scalar contribute. We compute the full 3 neutrino flavour evolution using the nusQUIDS code [53] and show the flavour transition probabilities in Fig. 5. For simplicity, we discuss the main features of interest assuming $|U_{\mu 4}| = |U_{\tau 4}|$ in a two-flavour approximation.

To a very good approximation, the flavour transitions of neutrinos in the Sun can be taken to be adiabatic [54]. In this limit, the relevant flavour conversion probabilities for a ν_α to convert into a ν_β , $P_{\alpha\beta}$, are approximately

$$P_{ee}(E_\nu) \approx c_{13}^4 \left(\frac{1}{2} + \frac{1}{2} \cos 2\theta_{12} \cos 2\theta_{12}^M \right) + s_{13}^4, \quad (\text{B1})$$

$$P_{\mu e}(E_\nu) + P_{\tau e}(E_\nu) = 1 - P_{ee}(E_\nu),$$

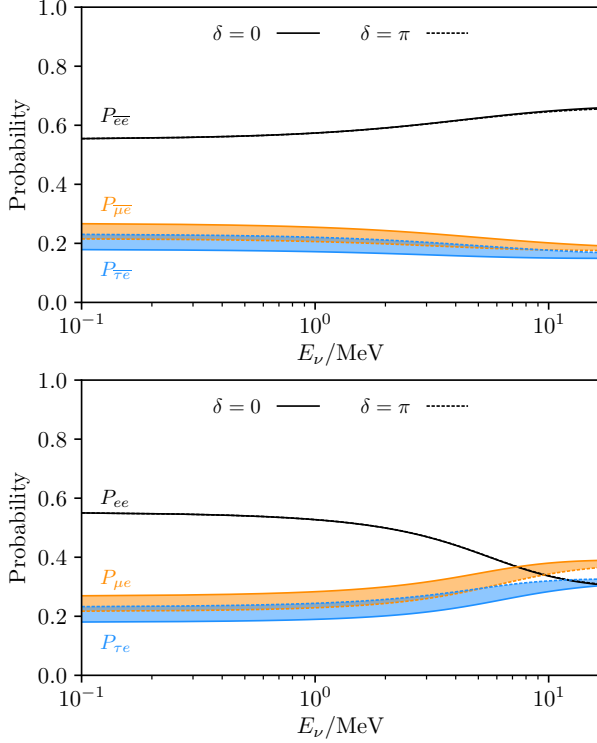


FIG. 5. Full flavour transition probabilities averaged over the neutrino production region for all flavours in the energy range of 0.1 to 17 MeV. The width of the band comes from varying $\delta \in [0, \pi]$.

with their antineutrino $P_{\alpha\bar{\beta}}$ analogue. Here, θ_{12}^M is the solar mixing angle in matter at the core, defined as

$$\tan 2\theta_{12}^M = \frac{\sin 2\theta_{12} \Delta m_{12}^2}{\Delta m_{12}^2 \cos 2\theta_{12} - A_{CC}}, \quad (\text{B2})$$

with $A = \pm 2\sqrt{2}E_\nu G_F N_e(0)$ for neutrinos (antineutrinos). It is easy to see that while ν_e states undergo the usual MSW transition, having enhanced flavour transi-

tions due to adiabatic conversions above the resonance, $P_{ee}(5 \text{ MeV}) \approx 0.32$, the $\bar{\nu}_e$ states do not. Instead, $\bar{\nu}_e$ change flavour less often above the resonance and have enhanced survival probabilities, $P_{\bar{e}\bar{e}}(5 \text{ MeV}) \approx 0.62$. The full flavour transition probability averaged over production region for ^8B neutrinos are shown in Fig. 5, where all channels involving a ν_e and $\bar{\nu}_e$ are shown for completeness.

Note that within a two-flavour approximation we can compute $P_{\mu\bar{e}}$ with no additional effort. This is because time reversal is a good symmetry in this case ($P_{\alpha\beta} = P_{\beta\alpha}$) as a consequence of the unitarity of the Hamiltonian, which holds even for non-symmetric matter profiles such as the Sun [53, 54]. Hence, the CPT asymmetry is equivalent to the CP asymmetry $P_{\alpha\beta} - P_{\alpha\bar{\beta}}$, such that $P_{\mu\bar{e}} = P_{e\bar{\mu}}$.

Appendix C: Statistical Method

When deriving upper limits on the mixing angles, we minimize the following log-likelihood function

$$\mathcal{L} = 2 \sum_i \left[\mu_i(\vec{\theta}, \vec{\beta}) - D_i + D_i \ln \frac{D_i}{\mu_i(\vec{\theta}, \vec{\beta})} \right] + \sum_{i,j} \frac{\beta_{i,j}^2}{\sigma_{i,j}^2}, \quad (\text{C1})$$

where $\vec{\theta}$ stands for the vector of physics parameters (*e.g.*, $|U_\alpha|^2$), $\vec{\beta}$ the vector of nuisance parameters with individual entries β_j and associated Gaussian errors σ_j . As an approximation, we assume \mathcal{L} to follow a χ^2 distribution when estimating our confidence intervals.

The most important systematics for our study are the uncertainties on the total ^8B solar neutrino flux and total backgrounds numbers. To be conservative, we assign each energy bin two normalisation systematics, one exclusive to the new physics prediction, modelling uncertainties in the solar flux, and one exclusive to backgrounds. All normalization systematics are assumed to be uncorrelated, which is conservative.

-
- [1] L. Wolfenstein, *Phys. Rev.* **D17**, 2369 (1978), [294(1977)].
 - [2] S. P. Mikheyev and A. Yu. Smirnov, *Sov. J. Nucl. Phys.* **42**, 913 (1985), [305(1986)].
 - [3] Y. Fukuda *et al.* (Super-Kamiokande), *Phys. Rev. Lett.* **81**, 1562 (1998), [arXiv:hep-ex/9807003 \[hep-ex\]](#).
 - [4] Q. R. Ahmad *et al.* (SNO), *Phys. Rev. Lett.* **89**, 011301 (2002), [arXiv:nucl-ex/0204008 \[nucl-ex\]](#).
 - [5] J. N. Bahcall, A. M. Serenelli, and S. Basu, *Astrophys. J. Suppl.* **165**, 400 (2006), [arXiv:astro-ph/0511337 \[astro-ph\]](#).
 - [6] M. Maltoni and A. Yu. Smirnov, *Eur. Phys. J.* **A52**, 87 (2016), [arXiv:1507.05287 \[hep-ph\]](#).
 - [7] S. Abe *et al.* (KamLAND), *Phys. Rev. Lett.* **100**, 221803 (2008), [arXiv:0801.4589 \[hep-ex\]](#).
 - [8] A. S. Joshipura, E. Masso, and S. Mohanty, *Phys. Rev.* **D66**, 113008 (2002), [arXiv:hep-ph/0203181 \[hep-ph\]](#).
 - [9] J. F. Beacom and N. F. Bell, *Phys. Rev.* **D65**, 113009 (2002), [arXiv:hep-ph/0204111 \[hep-ph\]](#).
 - [10] J. N. Bahcall, N. Cabibbo, and A. Yahil, *Phys. Rev. Lett.* **28**, 316 (1972), [285(1972)].
 - [11] S. Pakvasa and K. Tennakone, *Phys. Rev. Lett.* **28**, 1415 (1972).
 - [12] R. A. Malaney, B. S. Meyer, and M. N. Butler, *Astrophys. J.* **352**, 767 (1990).
 - [13] E. Vitagliano, J. Redondo, and G. Raffelt, *JCAP* **1712**, 010 (2017), [arXiv:1708.02248 \[hep-ph\]](#).
 - [14] E. K. Akhmedov, *Phys. Lett.* **B255**, 84 (1991).
 - [15] R. Barbieri, G. Fiorentini, G. Mezzorani, and M. Moretti, *Phys. Lett.* **B259**, 119 (1991).

- [16] B. Aharmim *et al.* (SNO), *Phys. Rev.* **D70**, 093014 (2004), [arXiv:hep-ex/0407029 \[hep-ex\]](#).
- [17] A. Gando *et al.* (KamLAND), *Astrophys. J.* **745**, 193 (2012), [arXiv:1105.3516 \[astro-ph.HE\]](#).
- [18] M. Agostini *et al.* (Borexino), (2019), [arXiv:1909.02422 \[hep-ex\]](#).
- [19] W. Linyan, *Experimental Studies on Low Energy Electron Antineutrinos and Related Physics*, Ph.D. thesis, Tsinghua University (2018), available at http://www-sk.icrr.u-tokyo.ac.jp/sk/_pdf/articles/2019/SKver-Linyan.pdf.
- [20] Y. Chikashige, R. N. Mohapatra, and R. D. Peccei, *Phys. Lett.* **98B**, 265 (1981).
- [21] G. B. Gelmini and M. Roncadelli, *Phys. Lett.* **99B**, 411 (1981).
- [22] Z. G. Berezhiani and M. I. Vysotsky, *Phys. Lett.* **B199**, 281 (1987), [,288(1987)].
- [23] Z. G. Berezhiani, G. Fiorentini, M. Moretti, and A. Rossi, *Z. Phys.* **C54**, 581 (1992).
- [24] C.-S. Lim and W. J. Marciano, *Phys. Rev.* **D37**, 1368 (1988), [,351(1987)].
- [25] E. K. Akhmedov, *Sov. Phys. JETP* **68**, 690 (1989), [*Zh. Eksp. Teor. Fiz.*95,1195(1989)].
- [26] S. Palomares-Ruiz, S. Pascoli, and T. Schwetz, *JHEP* **09**, 048 (2005), [arXiv:hep-ph/0505216 \[hep-ph\]](#).
- [27] Y. Bai, R. Lu, S. Lu, J. Salvado, and B. A. Stefanek, *Phys. Rev.* **D93**, 073004 (2016), [arXiv:1512.05357 \[hep-ph\]](#).
- [28] Z. Moss, M. H. Moulai, C. A. Argüelles, and J. M. Conrad, *Phys. Rev.* **D97**, 055017 (2018), [arXiv:1711.05921 \[hep-ph\]](#).
- [29] M. Dentler, I. Esteban, J. Kopp, and P. Machado, (2019), [arXiv:1911.01427 \[hep-ph\]](#).
- [30] A. de Gouvêa, O. L. G. Peres, S. Prakash, and G. V. Stenico, (2019), [arXiv:1911.01447 \[hep-ph\]](#).
- [31] R. M. Bionta *et al.*, *Phys. Rev. Lett.* **58**, 1494 (1987).
- [32] K. Hirata *et al.* (Kamiokande-II), *GRAND UNIFICATION. PROCEEDINGS, 8TH WORKSHOP, SYRACUSE, USA, APRIL 16-18, 1987*, *Phys. Rev. Lett.* **58**, 1490 (1987), [,727(1987)].
- [33] C. W. Kim and W. P. Lam, *Mod. Phys. Lett.* **A5**, 297 (1990).
- [34] K. Bays *et al.* (Super-Kamiokande), *Phys. Rev.* **D85**, 052007 (2012), [arXiv:1111.5031 \[hep-ex\]](#).
- [35] H. Zhang *et al.* (Super-Kamiokande), *Astropart. Phys.* **60**, 41 (2015), [arXiv:1311.3738 \[hep-ex\]](#).
- [36] C. H. Llewellyn Smith, *Gauge Theories and Neutrino Physics, Jacob, 1978:0175*, *Phys. Rept.* **3**, 261 (1972).
- [37] P. Vogel and J. F. Beacom, *Phys. Rev.* **D60**, 053003 (1999), [arXiv:hep-ph/9903554 \[hep-ph\]](#).
- [38] A. Strumia and F. Vissani, *Phys. Lett.* **B564**, 42 (2003), [arXiv:astro-ph/0302055 \[astro-ph\]](#).
- [39] A. M. Ankowski, (2016), [arXiv:1601.06169 \[hep-ph\]](#).
- [40] S. Horiuchi, J. F. Beacom, and E. Dwek, *Phys. Rev.* **D79**, 083013 (2009), [arXiv:0812.3157 \[astro-ph\]](#).
- [41] C. Lunardini, *Phys. Rev. Lett.* **102**, 231101 (2009), [arXiv:0901.0568 \[astro-ph.SR\]](#).
- [42] J. F. Beacom and M. R. Vagins, *Phys. Rev. Lett.* **93**, 171101 (2004), [arXiv:hep-ph/0309300 \[hep-ph\]](#).
- [43] C. Simpson *et al.* (Super-Kamiokande), *Astrophys. J.* **885**, 133 (2019), [arXiv:1908.07551 \[astro-ph.HE\]](#).
- [44] Y. S. Jeong, S. Palomares-Ruiz, M. H. Reno, and I. Sarcevic, *JCAP* **1806**, 019 (2018), [arXiv:1803.04541 \[hep-ph\]](#).
- [45] S. J. Li, J. J. Ling, N. Raper, and M. V. Smirnov, *Nucl. Phys.* **B944**, 114661 (2019), [arXiv:1905.05464 \[hep-ph\]](#).
- [46] F. An *et al.* (JUNO), *J. Phys.* **G43**, 030401 (2016), [arXiv:1507.05613 \[physics.ins-det\]](#).
- [47] J. F. Beacom *et al.* (Jinping), *Chin. Phys.* **C41**, 023002 (2017), [arXiv:1602.01733 \[physics.ins-det\]](#).
- [48] C. Boehm and P. Uwer, (2006), [arXiv:hep-ph/0606058 \[hep-ph\]](#).
- [49] A. Diaz, C. A. Argüelles, G. H. Collin, J. M. Conrad, and M. H. Shaevitz, (2019), [arXiv:1906.00045 \[hep-ex\]](#).
- [50] M. H. Moulai, C. A. Argüelles, G. H. Collin, J. M. Conrad, A. Diaz, and M. H. Shaevitz, (2019), [arXiv:1910.13456 \[hep-ph\]](#).
- [51] E. Bertuzzo, S. Jana, P. A. N. Machado, and R. Zukanovich Funchal, *Phys. Lett.* **B791**, 210 (2019), [arXiv:1808.02500 \[hep-ph\]](#).
- [52] P. Ballett, M. Hostert, and S. Pascoli, (2019), [arXiv:1903.07589 \[hep-ph\]](#).
- [53] A. de Gouvea, *Phys. Rev.* **D63**, 093003 (2001), [arXiv:hep-ph/0006157 \[hep-ph\]](#).
- [54] E. K. Akhmedov, P. Huber, M. Lindner, and T. Ohlsson, *Nucl. Phys.* **B608**, 394 (2001), [arXiv:hep-ph/0105029 \[hep-ph\]](#).